

Coassembly of Different Sulfonylurea Receptor Subtypes Extends the Phenotypic Diversity of ATP-sensitive Potassium (K_{ATP}) Channels

Adam Wheeler, Chuan Wang, Ke Yang, Kun Fang, Kevin Davis, Amanda M. Styer, Uyenlinh Mirshahi, Christophe Moreau, Jean Revilloud, Michel Vivaudou, Shunhe Liu, Tooraj Mirshahi, and Kim W. Chan

Department of Physiology and Biophysics, Case Western Reserve University, School of Medicine, Cleveland, Ohio (A.W., K.Y., K.F., K.D., S.L., K.W.C.); Weis Center for Research, Geisinger Clinic, Danville, Pennsylvania (C.W, A.M.S., U.M., T.M.); Institut de Biologie Structurale, Grenoble, France (C.M., J.R., M.V.).

Running title: Coassembly of two SUR subtypes form distinct K_{ATP} channels

Address correspondence: Kim W. Chan, Department of Physiology and Biophysics, Case Western Reserve University, School of Medicine, Cleveland, OH 44106-4970. Tel.: 216-368-0954; Fax: 216-368-1693; Email: kwc8@po.cwru.edu

Number of text pages: 29

Number of tables: 2

Number of figures: 9

Number of references: 39

Number of words in the *Abstract*: 250

Number of words in the *Introduction*: 638

Number of words in the *Discussion*: 1464

Abbreviations: ATP, Adenosine-5'-triphosphate; COS cells, African green monkey kidney fibroblast cells; diazoxide, 7-chloro-3-methyl-4H-1,2,4-benzothiadiazine 1,1-dioxide; DMSO, dimethyl sulfoxide; EDTA, ethylenediaminetetraacetic acid; EGTA, ethylene glycol-bis(2-aminoethylether)-N,N,N',N'-tetraacetic acid; ER, endoplasmic reticulum; glibenclamide, 5-chloro-N-[2-[4-(cyclohexylcarbamoylsulfamoyl)phenyl]ethyl]-2-methoxy-benzamide; HEPES, 4-(2-hydroxyethyl)-1-piperazineethanesulfonic acid; HEK cells, human embryonic kidney cells; Kir channel, inwardly rectifying potassium channel; pinacidil, 3-cyano-1-(4-pyridyl)-2-(1,2,2-trimethylpropyl)guanidine; SUR, sulfonylurea receptor

ABSTRACT

K_{ATP} channels are metabolic sensors and targets of potassium channel openers (KCO; e.g. diazoxide and pinacidil). They comprise four sulfonylurea receptors (SUR) and four potassium channel subunits (Kir6) and are critical in regulating insulin secretion. Different SUR subtypes (SUR1, SUR2A, SUR2B) largely determine the metabolic sensitivities and the pharmacological profiles of K_{ATP} channels. SUR1- but not SUR2-containing channels are highly sensitive to metabolic inhibition and diazoxide while SUR2-channels are sensitive to pinacidil. It is generally believed that SUR1 and SUR2 are incompatible in channel coassembly. We used triple tandems, T1 and T2, each containing one SUR (SUR1 or SUR2A) and two Kir6.2 Δ 26 (last 26 residues are deleted) to examine the coassembly of different SUR. When T1 or T2 was expressed in *Xenopus* oocytes, small whole-cell currents were activated by metabolic inhibition (induced by azide) plus a KCO (diazoxide for T1, pinacidil for T2). When coexpressed with any SUR subtype, the activated-currents were increased 2 to 13-fold, indicating that different SUR can coassemble. Consistent with this, heteromeric SUR1+SUR2A channels were sensitive to azide, diazoxide, pinacidil and their single-channel burst duration was 2-fold longer than that of the T1 channels. Furthermore, SUR2A was coprecipitated with SUR1. Using whole-cell recording and immunostaining, heteromeric channels could also be detected when T1 and SUR2A were coexpressed in mammalian cells. Finally, the response of the SUR1+SUR2A channels to azide was found to be intermediate to those of the homomeric channels. Therefore, different SUR subtypes can coassemble into K_{ATP} channels with distinct metabolic sensitivities and pharmacological profiles.

Introduction

Two characteristics, inhibition by intracellular ATP and activation by MgADP, define ATP-sensitive potassium (K_{ATP}) channels and underlie their ability to respond to metabolic changes inside a cell (Ashcroft, 2005; Masia *et al.*, 2005; Yamada and Inagaki, 2005). Under metabolic stress, their activity increases, resulting in hyperpolarization of the cell membrane which plays a critical role in cellular protection. Different K_{ATP} channels have different metabolic sensitivities (Schwappach *et al.*, 2000; Masia *et al.*, 2005). For example, the pancreatic K_{ATP} channels are usually partly open in normoglycemic conditions and are closed only when blood glucose levels become high. This property allows the pancreatic K_{ATP} channels to regulate insulin (Ashcroft, 2005). Cardiac K_{ATP} channels are closed under normal physiological states and open only when the cells are stressed, thus contributing towards the cardiac adaptive response to acute stress (Zingman *et al.*, 2002).

K_{ATP} channels comprise two subunits: the pore-forming inwardly-rectifying potassium (Kir6) channel subunit and the regulatory sulfonylurea receptor (SUR) subunit, an ATP-binding cassette (ABC) protein (Inagaki *et al.*, 1995). SUR primarily utilizes its unique N-terminal transmembrane domain, TMD0, to associate with Kir6 in a 4:4 stoichiometry to form the octameric K_{ATP} channel complex ($[SUR]_4[Kir6]_4$) (Shyng and Nichols, 1997; Clement *et al.*, 1997; Chan *et al.*, 2003; Babenko and Bryan, 2003). In mammals, there are two Kir6 and two SUR genes (*Kir6.1* and *Kir6.2*; *SUR1* and *SUR2*) (Aguilar-Bryan and Bryan, 1999; Shi *et al.*, 2005). SUR2 has two major splice variants, SUR2A and 2B, which differ only in the C-terminal 42 amino acids. It is believed that different Kir6 combine with different SUR to form the various native K_{ATP} channels. For example, the K_{ATP} channels found in the pancreas, striated muscle and smooth muscle are made up of SUR1+Kir6.2, SUR2A+Kir6.2 and SUR2B+Kir6.1/Kir6.2, respectively. SUR affects the responses of K_{ATP} channels to ATP and MgADP and is crucial in determining their metabolic sensitivities. The sensitivities to energy depletion of different K_{ATP} channels follow this order: SUR1+Kir6.2>>>SUR2B+Kir6.2>SUR2A +Kir6.2 (Masia *et al.*, 2005; Dabrowski *et al.*, 2003; Schwappach *et al.*, 2000; Liss *et al.*, 1999). SUR also serves as the main binding site for two important classes of drugs that target K_{ATP} channels: the sulfonylurea and potassium channel opener

(Gribble and Reimann, 2002; Moreau *et al.*, 2005). Different K_{ATP} channels exhibit different pharmacological profiles dictated by the SUR subtypes they are composed of.

It is generally believed that SUR1 cannot coassemble with SUR2 to form K_{ATP} channels (Giblin *et al.*, 2002; Tricarico *et al.*, 2006; Babenko, 2005), even though SUR1 and SUR2 share ~65% identity and are coexpressed in many cell types (Tricarico *et al.*, 2006; Baron *et al.*, 1999; Shi *et al.*, 2005; Liss *et al.*, 1999). We have recently demonstrated that a model in which SUR1 and SUR2A do not coassemble is incompatible with the properties of the macroscopic currents recorded from *Xenopus* oocytes expressing SUR1, SUR2A and Kir6.2 (Chan *et al.*, 2008). Furthermore, by coexpressing SUR1-Kir6.2 and SUR2A-Kir6.2(N160D) tandem dimers and studying the rectification properties of the resulting macroscopic currents, we found that SUR1 and SUR2A could coassemble, in a random manner, to form heteromeric K_{ATP} channels. Here, we report our further study on the coassembly of different SUR subtypes and explore the resulting functional consequences. First, we show SUR2A and Kir6.2 were coprecipitated with SUR1 when all three proteins were coexpressed in *Xenopus* oocytes. Second, by using two triple tandems in which one SUR is linked to two Kir6.2 Δ 26 (the region comprising the last 26 amino acids in Kir6.2 contains an ER retention sequence and is deleted) (Fig. 2A), we show that SUR1, SUR2A and SUR2B could coassemble in all the possible pair-wise combinations. Third, we demonstrate that K_{ATP} channels comprising two different SUR subtypes displayed hybrid pharmacological properties and novel metabolic sensitivities. Last, we demonstrate that heteromeric K_{ATP} channels were also formed in mammalian cells cultured at 37 °C.

Materials and Methods

Molecular biology. A SalI site was introduced after the last sense codon in SUR1 (in pGEMHE) by Quickchange mutagenesis (Stratagene). The Kir6.2 Δ 26 dimeric cassette was generated by PCR and subcloned into pGEMHE. SUR1 was then excised using BamHI and SalI and inserted before the Kir6.2 Δ 26 dimeric cassette to produce the SUR1-Kir6.2 Δ 26-Kir6.2 Δ 26 triple tandem (T1). The peptide sequences of linker 1 (between SUR and Kir6.2 Δ 26) and linker 2 (between adjacent Kir6.2 Δ 26) in T1 are

VDGRG₈DI and NSRG₈DI, respectively. An XbaI site was introduced after the last sense codon of SUR2A which was then excised using XbaI and inserted before the Kir6.2Δ26 dimeric cassette to produce the SUR2A-Kir6.2Δ26-Kir6.2Δ26 triple tandem (T2). The peptide sequence of linker 1 in T2 is SRVRRYGRG₈DI. The SUR1 in T1 has a FLAG tag at its N-terminus. The GFG sequence in the selectivity filter of Kir6.2Δ26 was mutated to AAA in either cassette I or cassette II of the Kir6.2Δ26 dimeric construct. SUR1 was then inserted to generate T1(I-AAA) and T1(II-AAA). GFP was appended to the C-terminus of Kir6.2 to create Kir6.2-GFP. SUR1-HA and SUR2-HA were generated by inserting an HA-epitope in the last extracellular loop (between TM16 and TM17) (Zerangue *et al.*, 1999). FLAG-SUR1 (F-SUR1) has been described (Yang *et al.*, 2005). cRNA were synthesized by in vitro transcription and their concentrations were estimated on agarose gels from the relative intensities of the RNA bands with respect to a calibrated RNA marker.

Oocyte preparation, two-electrode voltage clamp and inside-out patch clamp recordings. *Xenopus laevis* oocytes were prepared and cultured at 18 °C as described and all animal procedures were in accord with the IACUC (Chan *et al.*, 2003). 2 ng of T1 or T2 with or without 3 ng of SUR1, SUR2A or SUR2B were injected into oocytes for two-electrode voltage clamp (TEVC), Western blot and immunoprecipitation. The same T1 and T1+SUR2A RNA solutions were then diluted 5-20 times for single-channel recording. TEVC was used to measure whole-cell currents from *Xenopus* oocytes using an OC-725 amplifier (Warner). Bath solution contains (in mM): 96 KCl, 2 NaCl, 1 MgCl₂, 5 HEPES, 1.8 CaCl₂ (pH 7.5). 3M sodium azide (in water; Sigma), 340 mM diazoxide (in DMSO; Sigma), 200 mM pinacidil (ethanol; Sigma), 20 mM glibenclamide (DMSO; Sigma) and 1 M BaCl₂ (water) were used as stocks. To monitor whole-cell conductance, oocyte membrane was held at 0 mV and 1-s ramps from -100 to +100 mV were applied at 1.5-s interval. Currents were filtered at 1 kHz and sampled at 2 kHz. Currents at -80 mV from the ramp were used to plot the time courses and for comparing current magnitudes. An Axopatch 200B amplifier (Molecular Devices) was used for patch clamping in the inside-out configuration. Pipette solution contained (in mM) 140 KCl, 1 MgCl₂, 1 CaCl₂ and 10 HEPES (pH 7.4).

Bath solution contained 140 KCl, 1 EGTA, 1 EDTA and 10 HEPES (pH 7.4). Single channel recordings were obtained at -60 mV and the currents were filtered at 2 kHz and sampled at 25 kHz. Pipette resistances were 3-5 MΩ. Analyses of single channel records were performed as previously described, using a combination of pCLAMP 9 and in-house programs (Fang *et al.*, 2006). The open-time and closed-time distributions obtained from single channel records were best fitted by 1 and 4 exponentials, using maximum likelihood. τ_{ci} and a_{ci} are the time constant and the fractional contribution of the i^{th} closed time component, respectively ($i=1-4$). τ_o is the *true* mean open time obtained from the *observed* mean open time ($\tau_{o,obs}$) after correction for the filter dead time ($t_d \approx 0.09$ ms); i.e., $\tau_o = \tau_{o,obs} * e^{-t_d/\tau_{c1}}$ (Fang *et al.*, 2006). The number of channel closures within a burst (N), the burst duration (τ_b) and the interburst duration (τ_{ib}) were calculated as follows.

$$N = \frac{a_{c1}}{(a_{c2} + a_{c3} + a_{c4})} = \frac{a_{c1}}{1 - a_{c1}}$$

$$\tau_b = (N+1) * \tau_o + N * \tau_{c1}$$

$$\tau_{ib} = (a_{c2} * \tau_{c2} + a_{c3} * \tau_{c3}) / (a_{c2} + a_{c3})$$

All electrophysiological data were obtained at room temperature (25 °C) and are given as mean \pm S.E.M ($n \geq 5$).

Oocyte crude membrane preparation, Western blot analysis and immunoprecipitation. Oocyte crude membranes were prepared 2-3 days post-injection, as described previously (Chan *et al.*, 2003). Resuspended crude membrane proteins were mixed with standard sample loading buffer at room temperature without heating and were resolved on SDS-polyacrylamide gels and transferred to nitrocellulose membranes for Western blot analyses using the anti-HA (Roche; from rat), or anti-FLAG (Sigma; M2, from mouse) or anti-GFP antibodies (Molecular Probes; from mouse). Crude membranes were solubilized in 1% digitonin (Calbiochem) or Triton (Sigma) and immunoprecipitations were performed using M2 antibodies conjugated to agarose beads (Sigma).

Expression and whole-cell recordings in COS-7 cells. COS-7 cells were cultured at 37 °C in MEM supplemented with 10% FBS. T1, SUR1-HA, SUR2A-HA and Kir6.2-HA were subcloned into pcDNA3. Cells were transfected using Lipofectamine2000 (Invitrogen) with the following amounts of DNA for different constructs, as indicated for each experiment: 2 µg T1, 1.6 µg SUR1-HA, 1.6 µg SUR2A-HA, 0.1 µg pEGFP-N1 (Clontech). Patch clamp recordings were made 36-72 hrs post-transfection. Glass coverslips containing transfected cells were placed in a chamber which was constantly superfused with high potassium (HK) solution with the following composition (mM): 140 KCl, 2.6 CaCl₂, 1.2 MgCl₂, 5 HEPES (pH 7.4). Whole-cell patch clamp recordings were performed at room temperature by using a MultiClamp700B amplifier (Molecular Devices). Pipettes were filled with (mM): 140 KCl, 1.2 MgCl₂, 1 CaCl₂, 10 EGTA, 5 HEPES (pH 7.4) supplemented with 3 mM Mg-ATP; and typical resistances were 3-6 MΩ. Cells were held at 0 mV and a 475 ms ramp from -100 mV to +100 mV was applied once every 0.5 s or 2 s. Whole cell capacitance was fully compensated. Currents were filtered at 1 kHz and sampled at 2 kHz. Currents at -80 mV from the ramp were used to plot the time courses and for comparing current magnitudes.

Immunocytochemistry. HEK-293 cells were plated at a density of 5x10⁵ cells per plate on polylysine-treated 35 mm glass bottom dishes. On the following day the cells were transiently transfected with SUR1-HA, or SUR2A-HA (0.5 µg each) with or without T1 (0.625 µg) as well as a CFP-tagged membrane marker (CFP fused to the first 20 amino acids of GAP-43; Clontech). Control cells were transfected using empty pcDNA3 vector. Transfected cells were fixed using 4% paraformaldehyde and permeabilized using 0.05% Triton-X100. The cells were stained with rat anti-HA (Roche) followed by AlexaFluor594-conjugated chicken anti-rat-IgG (Invitrogen). Cells were washed extensively using PBS and imaged using a spinning disk confocal microscope (Olympus). All images were processed using IPlab softwar (Scanalytics).

Results

Coprecipitation of SUR2A and Kir6.2 with SUR1. If SUR1 and SUR2A can coassemble with Kir6.2 to form heteromeric K_{ATP} channels, both SUR2A and Kir6.2 should be coprecipitated with SUR1. To test this, SUR1 (FLAG-tagged) was expressed with Kir6.2 (GFP-tagged) and SUR2A (HA-tagged) or SUR1 (HA-tagged) in *Xenopus* oocytes (Fig. 1; lanes 1 & 2 from left). The same combinations of proteins were also expressed but an untagged SUR1 was used to replace the F-SUR1 (lanes 3 & 4). Western blots showed that F-SUR1, SUR1-HA or SUR2A-HA, and Kir6.2-GFP were expressed in the crude oocyte membranes (Figs. 1A, B & C). When F-SUR1 was immunoprecipitated, the coexpressed SUR1-HA or SUR2A-HA and Kir6.2-GFP were all identified in the immunoprecipitates (Figs. 1D & E; lanes 1 & 2; n=3). Coprecipitations of SUR1-HA or SUR2A-HA and Kir6.2-GFP required the presence of the FLAG tag in SUR1 (Figs. 1D & E; lanes 3 & 4). Removing the GFP tag in Kir6.2 did not affect the coprecipitation of SUR2A with SUR1 (data not shown). These data indicate that both SUR2A and Kir6.2 are coimmunoprecipitated with SUR1, consistent with the idea that SUR1, SUR2A and Kir6.2 are present in the same multimeric-channel complex.

Triple tandems as probes of the subunit composition of K_{ATP} channels. We constructed two triple tandems, T1 and T2, to investigate whether any two of the three SUR subtypes (SUR1, SUR2A and SUR2B) could coassemble and to study the pharmacology and the metabolic sensitivities of heteromeric K_{ATP} channels comprising two different SUR subtypes. T1 and T2 were constructed by connecting SUR1 and SUR2A, respectively, and two Kir6.2 Δ 26 cassettes through glycine linkers (Fig. 2A). Using *Xenopus* oocytes, T1 and T2 were expressed alone or with different SUR. Whole-cell currents were recorded from oocytes using two-electrode voltage clamp (TEVC). As shown in Figure 3A, oocytes expressing T1 exhibited a small basal current which could be further activated by sodium azide, a metabolic inhibitor which increases the amount of intracellular ADP at the expense of ATP (Gribble *et al.*, 1997). Current from T1 could also be activated by diazoxide, a potassium channel opener (KCO) specific for SUR1 and SUR2B, but not by pinacidil, a KCO specific for SUR2. A switch from diazoxide to pinacidil caused a reduction in the current, which can be explained by the removal of diazoxide from the bath solution.

~70% of the total current (I_{tot} ; see Fig. 3 and legend for definition) could be inhibited by 10 μM glibenclamide and the remaining current could be blocked by Ba^{2+} . These data indicate that T1 can form functional channels with characteristics similar to the K_{ATP} channels formed by SUR1 and Kir6.2 Δ 26 (data not shown). However, the magnitude of the current at maximal activation ($I_{\text{tot}} = -3.70 \pm 0.7 \mu\text{A}$; $n=8$) was much smaller compared to SUR1+Kir6.2 Δ 26 ($I_{\text{tot}} = -52 \pm 6 \mu\text{A}$; $n=11$), suggesting that T1 alone is inefficient in forming functional K_{ATP} channels. It is noteworthy that the glibenclamide sensitivity of the T1 channels was less than that of the SUR1+Kir6.2 Δ 26 channels (~97% of I_{tot} was inhibited by 10 μM glibenclamide for SUR1+Kir6.2 Δ 26; $n=5$). A possible reason that T1 could be functionally expressed in oocytes is the absence of the ER retention sequence in the Kir6.2 Δ 26 subunit. Figure 2B shows some possible assembly configurations for functional channels formed by T1 alone. It is clear that all the configurations shown represent channels with either impaired stoichiometry and/or with serious steric hindrance.

Next, we coexpressed T1 and SUR1 to investigate whether they could assemble. Oocytes expressing T1+SUR1 exhibited much larger basal currents compared to those expressing T1 alone (Fig.3B & Table 1). The basal current was robustly activated by azide and diazoxide. A switch from diazoxide to pinacidil again led to a small reduction in the current. Glibenclamide promptly inhibited ~90% of the activated current and the remaining small current was blocked by Ba^{2+} . The characteristics and the magnitude of the currents resulting from T1+SUR1 were similar to those from oocytes expressing SUR1+Kir6.2 Δ 26 (For T1+SUR1, $I_{\text{tot}} = -31.24 \pm 4.64 \mu\text{A}$; $n=8$). Importantly, the basal and the total currents were 6- and 8-fold larger compared to those from oocytes expressing T1 alone (Fig. 3E and Table 1). As a control, when T1 was expressed with MRP1, another TMD0-containing ABC protein, the resulting basal and total currents were only $-0.19 \pm 0.17 \mu\text{A}$ and $-1.87 \pm 0.11 \mu\text{A}$, respectively (Table 1). These data indicate that freely expressed SUR1, but not MRP1, can assemble with T1 to enhance the formation of functional channels.

We then investigated whether the functional channels formed when T1 was coexpressed with SUR1 utilized as expected the two Kir6.2 Δ 26 cassettes of T1. Two mutants, T1(I-AAA) and T1(II-AAA), with

the conserved GFG pore-loop sequence mutated to AAA in cassette I and II, respectively, were designed (Fig. 2A). These Kir6.2 pore mutations have a dominant negative effect within the tetrameric K_{ATP} channel (Pountney *et al.*, 2001). Although both mutant proteins were expressed at a level similar to the wild-type T1 (Western blot not shown), neither mutant generated detectable stimulated currents when coexpressed with SUR1 ($I_{tot} = -1.3 \pm 0.3 \mu A$ and $-1.4 \pm 0.2 \mu A$ for I-AAA+SUR1 and II-AAA+SUR1, respectively; $n=5$). This observation suggests that the two Kir6.2 in T1 equally participate in the formation of the channels that we were recording and that the stoichiometry of the T1+SUR1 channels is $[SUR1]_2[SUR1-(Kir6.2\Delta26)]_2$ and therefore does not deviate from the wild-type octameric structure.

Using the triple tandem construct T1 to study the coassembly of SUR1 and SUR2. To address whether SUR2A and SUR2B could assemble with T1 to form functional channels, T1 was coexpressed with SUR2A and SUR2B and the basal and activated currents were measured (Figs. 3C & D). Oocytes expressing T1+SUR2A and T1+SUR2B exhibited small basal currents which could be stimulated by azide and diazoxide. Compared to T1 alone, the basal currents for T1+SUR2A and T1+SUR2B were about twice larger and currents activated by azide plus diazoxide (i.e. $I_{az}+I_{dzo}$) were ~4- and 6-fold larger, respectively (Fig. 3E & Table 1). We also found that SUR2A, when coexpressed with T1(I-AAA) or T1(II-AAA), did not produce any significant activated currents ($<-1.4 \mu A$; $n=10$). These data indicate that T1 (i.e. SUR1) can also coassemble with SUR2A and SUR2B to generate K_{ATP} channels with SUR1 properties. The most likely stoichiometry of these coassembled channels is $[SUR2]_2[SUR1-(Kir6.2\Delta26)]_2$ and the two possible configurations for SUR1-SUR2 hybrid channels are shown in Figure 2C. We tested whether these hybrid channels display SUR2-specific properties. Indeed, current from T1+SUR2A could be robustly activated by pinacidil (~60% of the total current) (Fig. 3C). As a result, the total current from T1+SUR2A was comparable to that of T1+SUR1 and was ~8-fold larger than that of T1 alone (Fig. 3E & Table 1). Even in the absence of prior azide preconditioning, pinacidil could still activate T1+SUR2A channels, albeit much less effectively (data not shown). Interestingly, pinacidil failed to activate the current from T1+SUR2B (Fig. 3D), even though it can activate SUR2B+Kir6.2 Δ 26 (data

not shown). Nevertheless, these data indicate that it is possible for SUR2A to assemble with SUR1 to generate K_{ATP} channels with both SUR1- (azide and diazoxide sensitivities) and SUR2A-specific (pinacidil activation) properties.

The triple tandem construct T1 can physically associate with both SUR1 and SUR2A. We further tested whether SUR1 and SUR2A could associate with T1 by performing immunoprecipitation. T1 (FLAG-tagged) was expressed alone, with SUR1 and with SUR2A (both were HA-tagged) (Fig. 4). We first performed Western blot to show the expression of each protein. Figure 4A shows a Western blot for T1 and F-SUR1 (included as a control). Three bands were detected for SUR1, which ran at ~160, 280 and 500 kDa. These bands are likely to represent the monomeric, dimeric and trimeric forms of SUR1 (predicted sizes are 178, 356 and 534 kDa, respectively), with the middle band running anomalously at a size much smaller than the predicted MW of a dimer. T1 was detected as two bands running at ~190 and 500 kDa that could represent its monomers and dimers (predicted sizes are 262 and 524 kDa), with the lower band running anomalously at a size smaller than that predicted for a monomer. SUR1 and SUR2A could also be detected in the blot when probed with the anti-HA antibody (Fig 4B). For each protein, the signal appeared as a sharp band and a trailing smear. As shown before, these represent the core- and mature-glycosylated forms of the SUR protein, respectively (Yang *et al.*, 2005; Zerangue *et al.*, 1999). T1 must enhance the formation of the mature-glycosylated form of SUR because the trailing smear was absent when SUR was expressed alone (Fig. 4A). Immunoprecipitation of T1 was then performed using the anti-FLAG antibody. Both the core- and mature-glycosylated forms of SUR1 and SUR2A were coprecipitated (Fig. 4C). These data indicate that T1 physically associates with SUR1 and SUR2A, in agreement with the electrophysiological experiments.

Incorporation of SUR2A into T1 results in longer burst durations. We asked whether the incorporation of SUR into T1 channels would affect the single channel properties of T1. To this end, we focused on T1 and T1+SUR2A channels for two reasons. First, it has been shown that both the intrinsic open probability (P_o) and the burst duration of SUR2A+Kir6.2 are larger compared to SUR1+Kir6.2 (Babenko *et al.*, 1999; Fang *et al.*, 2006). We reasoned that SUR2A would have a larger observable effect

on the single channel properties of T1 than SUR1. Second, we were most interested in whether SUR1 and SUR2A could coassemble. Figure 5A shows representative single channel recordings for T1 and T1+SUR2A channels. T1 and T1+SUR2A had identical single channel conductance (~ 58 pS at -60 mV; Table 2) and their open and closed times were best fitted with 1 and 4 exponentials, respectively (Fig. 5B). Their intra-burst kinetics, as revealed by the fastest closed time (τ_{c1}) and the open time (τ_o), their mean inter-burst closed times (τ_{ib}), and P_o , were not significantly different (at $p < 0.05$; Table 2). However, the mean burst duration for T1+SUR2A was ~ 2 -fold longer than that of T1 (280 ms versus 123 ms; $p < 0.015$). These data further indicate that SUR2A can associate with T1 to form heteromeric channels with longer burst duration.

Using the triple tandem construct T2 to study the coassembly of different SUR subtypes. As shown above, T1 can be used to test whether SUR1 can assemble with SUR2A and SUR2B. However, T1 cannot be used to address whether SUR2A can assemble with SUR2B. T2 was constructed specifically for this aim (Fig. 2A). Similar to T1, T2 could form functional channels when expressed in oocytes (Fig. 6A). Basal current from T2 was small and insensitive to azide and diazoxide but could be stimulated by pinacidil. The stimulated current was sensitive to glibenclamide and Ba^{2+} . When T2 was coexpressed with SUR1 or with SUR2A, the currents activated by pinacidil were 12- and 3-fold larger compared to that measured for T2 alone, respectively (Fig. 6 & Table 1). In addition, T2+SUR1, but not T2+SUR2A, were sensitive to azide and diazoxide (Figs. 6B, C, E). When T2 was coexpressed with SUR2B, the current activated by pinacidil was ~ 2 -fold larger compared to that measured for T2 alone (Fig. 6D & Table 1). Azide could not stimulate current from T2+SUR2B but diazoxide could clearly cause a small activation. These data demonstrate that T2 could assemble with SUR1, SUR2A and SUR2B leading to an increase in the pinacidil-activated currents (Fig. 6E & Table 1). Diazoxide sensitivity was also conferred by SUR1 and SUR2B but azide stimulation was observed only in the presence of SUR1.

T1 can assemble with SUR1 or SUR2A to form functional K_{ATP} channels in mammalian expression system. Our data presented so far were obtained from *Xenopus* oocytes cultured at 18 °C. To address

whether SUR1 and SUR2A could coassemble to form functional heteromeric channels in mammalian cells at 37 °C, we expressed T1, T1+SUR1 and T1+SUR2A in COS-7 cells and performed whole-cell recordings. Currents from COS-7 cells expressing SUR1+Kir6.2 and SUR2A+Kir6.2 were characterized first and found to display typical subtype-specific activation by KCOs. Additionally, the latter but not the former currents were reversibly inhibited by glibenclamide (data not shown). In cells expressing T1 alone or T1+SUR1 (Figs 7A-B), diazoxide but not pinacidil, was able to activate the currents, which could be inhibited by glibenclamide and the remaining currents could be blocked by Ba²⁺. After a 5-min wash with HK solution, application of diazoxide could not re-activate the currents. Hence, T1 alone or T1+SUR1 could form functional K_{ATP} channels with properties similar to SUR1+Kir6.2. However, the mean current density of T1+SUR1 ($I_{tot}=133\pm 22$ pA/pF; n=6) was ~3-fold larger than that of T1 alone ($I_{tot}=43\pm 7$ pA/pF; n=5) (Figs. 7A, B and 7D). These data are consistent with our findings in oocytes (Fig. 2) and reports that showed irreversible glibenclamide block of SUR1+Kir6.2 channels (Giblin *et al.*, 2002; Gribble *et al.*, 1997). Figure 7C shows the current from a cell expressing T1+SUR2A, which could be activated by diazoxide and further activated by pinacidil. Both activated currents could be inhibited by glibenclamide. Hence T1+SUR2A can generate K_{ATP} currents in COS-7 cells with characteristics qualitatively identical to those from oocytes expressing T1+SUR2A, indicating that functional heteromeric SUR1-SUR2A channels can also be formed in COS-7 cells. The cell shown in Figure 7C was subsequently washed for 5 minutes. After washing, the currents could not be re-activated by diazoxide but were readily re-activated by pinacidil, which could be subsequently inhibited by glibenclamide (Fig. 7C). The mean current density from the second pinacidil application (29 ± 7 pA/pF; n=6) was ~65% of that from the first application (45 ± 1 pA/pF; n=6) (Fig. 7D). Summary of the recordings from all three groups are shown in Figure 7D.

Next, we examined the changes in the surface localization of SUR1 and SUR2A in HEK-293 cells when they were expressed alone and with T1 (SUR1 and SUR2A were HA-tagged). When expressed alone, SUR1 and SUR2A proteins were mostly intracellularly located (Figs. 8A & C). In the presence of T1, both SUR1 and SUR2A were largely detected on the cell surface (Figs. 8B & D). Cells transfected

with empty vector and those where the primary antibody was left out were used as negative controls (Figs. 8E-F). For all immunofluorescence experiments a CFP-tagged membrane marker was co-transfected and imaged to clearly identify the plasma membrane (not shown). These data suggest that heteromeric K_{ATP} channels containing both SUR1 and SUR2A are largely located in the cell membrane when expressed in HEK-293 cells.

K_{ATP} channels comprising SUR1 and SUR2A show intermediate response to metabolic inhibition.

Do the hybrid K_{ATP} channels formed by SUR1 and SUR2 respond differently to metabolic inhibition compared to the channels formed by only SUR1 and SUR2? To examine this, we compared the rate, the extent and the concentration dependence of azide activation of channels formed from T1+SUR1 and T1+SUR2, when expressed in *Xenopus* oocytes. At 3 mM azide, the times required to reach half-maximal response ($t_{1/2}$) for T1+SUR1 and SUR1+Kir6.2 Δ 26 were not significantly different (308 ± 12 s versus 277 ± 16 s). The $t_{1/2}$ for T1+SUR1 was smaller than that for T1+SUR2B (366 ± 12 s; $p < 0.01$) which was in turn smaller than that for T1+SUR2A (418 ± 14 s; $p < 0.03$) (Fig. 9A). The extent of azide activation was highest for T1+SUR1. At 3 mM azide, the activated current was ~2- and 3-fold larger compared to that activated for T1+SUR2B and T1+SUR2A, respectively (Table 1); at a saturating concentration of 5 mM, azide stimulated T1+SUR1 ~5-fold more than T1+SUR2A (data not shown). Figure 9B shows the representative time courses of the normalized currents obtained from T1+SUR1 and T1+SUR2A in the sequential presence of two different doses of azide (1 mM followed by 5 mM). The ratio of the current response to 1 mM over that to 5 mM azide was 0.43 ± 0.07 ($n=5$) for T1+SUR1, which was ~2.5-fold higher than for T1+SUR2A (ratio= 0.16 ± 0.03 ; $n=5$), indicating that T1+SUR1 was more sensitive to azide activation. Taken together, the rate and extent of activation by metabolic inhibition of the SUR1-SUR2 hybrid channels were intermediate, between those of SUR1 channels (large rapid activation and higher sensitivity to low dose of metabolic inhibitor) and SUR2A channels (no detectable activation).

Discussion

Although Giblin *et al.* could not find evidence that SUR1 and SUR2 could interact (Giblin *et al.*, 2002), other reports suggested/indicated that different SUR subtypes could coassemble to form functional K_{ATP} channels. First, both SUR1 and SUR2 were detected in neonatal rat atrial myocytes whose single K_{ATP} channels revealed both SUR1 and SUR2 properties (Baron *et al.*, 1999). Second, three dopaminergic neuronal populations, expressing Kir6.2 with SUR1, SUR1+SUR2B and SUR2B, displayed K_{ATP} currents with high, intermediate and low sensitivities, respectively, to tolbutamide and metabolic inhibition (Liss *et al.*, 1999). Importantly, the currents with intermediate tolbutamide sensitivity were best fitted with only a single Hill equation, a result more consistent with a single population of heteromeric channels than with a mixed population of homomeric channels. Third, the attenuations of cardiac K_{ATP} currents by antisense oligodeoxynucleotides directed against SUR1 or SUR2 or both suggested the presence of native SUR1-SUR2 hybrid channels (Yokoshiki *et al.*, 1999). Amidst such controversy, we recently showed that SUR1 and SUR2A coassemble readily and randomly to form heteromeric K_{ATP} channels (Chan *et al.*, 2008). Here, we further demonstrate that SUR1, SUR2A and SUR2B can coassemble in all the possible pairwise combinations to form functional K_{ATP} channels with distinct properties, resulting in an increase in their functional and pharmacological diversity. To our knowledge, this is also the first report on the heteromerization of two similar but distinct full-length ABC transporter proteins into functional complexes. Furthermore, using a tandem dimer strategy, we have obtained evidence supporting the existence of heteromeric SUR1-SUR2A-Kir6.1-Kir6.2 channels in a heterologous expression system (see Supplemental Figure).

SUR1 can coassemble with SUR2A in *Xenopus* oocytes and in mammalian cells. There were six lines of evidence indicating that SUR1 can coassemble with SUR2A in *Xenopus* oocytes. First, the azide plus diazoxide activated currents from the T1+SUR2A channels were ~4-fold larger than those from the T1 channels (Figs. 3A, C & E). Similarly, the azide plus pinacidil activated currents from the T2+SUR1 channels were ~13-fold larger than those from the T2 channels (Figs. 6A, B & E). This might be due to an increase in the number of channels expressed on the cell membrane, because the ATP sensitivities (data

not shown) and the P_o of the T1 and T1+SUR2A channels were similar. Second, SUR2A could associate with T1 and become maturely glycosylated (Figs. 4B & C). This indicates that the T1-SUR2A complex can transit from the ER to the Golgi bodies and finally traffic to the cell membrane. Third, the T1+SUR2A and the T2+SUR1 channels were sensitive to pinacidil (SUR2-specific) in addition to azide and diazoxide (SUR1-specific) (Figs. 3C & 6B). Fourth, the glibenclamide sensitivities of the T1+SUR2A and T2+SUR1 channels were higher than those of the T1 and T2 channels by themselves (Table 1). This is consistent with the idea that any SUR subtype can incorporate into T1 and T2 thereby increasing their glibenclamide sensitivities. Fifth, SUR2A could increase the burst duration of T1 by 2-fold (Fig. 5 and Table 2), consistent with SUR2A assembling with and prolong the burst durations of single T1 channels (Babenko *et al.*, 1999; Fang *et al.*, 2006). Last, in the presence of Kir6.2, SUR2A could associate with SUR1 even when all three proteins were expressed separately (Fig. 2). These immunoprecipitation data are in contrast with the results presented by Giblin *et al.* who concluded that SUR1 could not coprecipitate SUR2A. This discrepancy may be due to the different expression systems used (*Xenopus* oocytes versus HEK-293 cells) and the different antibodies employed in the immunoprecipitations (anti-FLAG versus anti-SUR antibodies). Nevertheless, the positive biochemical data we obtained are consistent with our functional data strongly supporting the notion that SUR1 and SUR2 do coassemble. It is also noteworthy that in our immunoprecipitation experiment, a positive control in which SUR1-HA was coimmunoprecipitated with F-SUR1 was included.

The pharmacological characteristic of the whole-cell currents recorded from COS-7 cells expressing T1+SUR2A was qualitatively similar to that recorded from oocytes expressing T1+SUR2A (Figs 3C and 7C), demonstrating that heteromeric SUR1-SUR2A channels can also be formed in mammalian cells cultured at 37 °C. Interestingly, heteromeric SUR1-SUR2A channels could be re-activated by pinacidil (but not by diazoxide) after a 5 min wash-out of glibenclamide (Fig. 7). The mean ratio of the second pinacidil response to the first response was less than 1 (0.65), which might be due to current run-down. These data provide novel insights into the complex interaction between different KCOs and sulfonylurea, challenging the assumption that heteromeric SUR1-SUR2A channels cannot be activated by SUR2-

specific openers after a 5 min wash-out of the high affinity glibenclamide (Giblin *et al.*, 2002). Such assumption led Giblin *et al.* to interpret one of their experimental results as evidence that SUR1 and SUR2A cannot coassemble. The immunostaining data obtained from HEK-293 cells indicate that T1 can interact with SUR1 and SUR2A and chaperone them to the cell surface (Fig. 8). The strikingly similar staining patterns of SUR1 and SUR2A in the absence or the presence of T1 further suggest that the SUR1 subunit within T1 associates with a free SUR1 or SUR2A subunit in a non-discriminate manner. Using the voltage-dependent spermine blocker, we have demonstrated that the tandem dimers SUR1-Kir6.2 (a weak rectifier) and SUR2A-Kir6.2(N160D) (a strong rectifier) coassemble to form functional K_{ATP} channels in a random manner (Chan *et al.*, 2008).

SUR2B can coassemble with SUR1 and SUR2A. SUR2B, like SUR2A, boosted the T1 channel expression: the (azide+diazoxide)-activated current from T1+SUR2B was ~6.5-fold larger than that from T1. This potentiating effect of SURB on T1 was even stronger than that of SUR2A (~4-fold). Therefore, SUR2B must be able to assemble with SUR1 at least as well as SUR2A. Surprisingly, T1+SUR2B channels were not sensitive to pinacidil, although the SUR2B+Kir6.2 channels are activated by pinacidil as well as, if not better than, the SUR2A+Kir6.2 channels (data not shown) (Shindo *et al.*, 1998). This suggests a difference in the way SUR2A and SUR2B interact with SUR1. SUR2A and SUR2B are 98% identical and while it is generally believed that they can coassemble (Giblin *et al.*, 2002; Tricarico *et al.*, 2006), this interaction has not been directly demonstrated. Our data on T2+SUR2B provide clear evidence of their coassembly. First, the total current for T2+SUR2B was ~2-fold larger compared to the T2 channels. Although this relative increase was modest, it was comparable to that of the T2+SUR2A channels (~3-fold). Second, unlike T2+SUR2A, the T2+SUR2B channels could be clearly activated by diazoxide, although the activation was relatively small and variable. These data are in line with the diazoxide responses of wild-type SUR2B+Kir6.2 and SUR2A+Kir6.2 channels (Matsuoka *et al.*, 2000).

Physiological, pharmacological and mechanistic significance of coassembly of different SUR subtypes. It has been shown that the Kir6.1 and Kir6.2 are coexpressed in many tissues and they can form heteromers (Thomzig *et al.*, 2005; Karschin *et al.*, 1997; Babenko *et al.*, 2000; Cui *et al.*, 2001).

However, the biological significance of this coassembly is unclear because Kir6.1 and Kir6.2 have similar ATP sensitivities (Babenko and Bryan, 2001). On the other hand, the heteromerization of SUR has obvious implications on cellular functions, because the metabolic sensitivity, the most important physiological property of K_{ATP} channels, is largely determined by SUR (Masia *et al.*, 2005; Schwappach *et al.*, 2000; Dabrowski *et al.*, 2003; Liss *et al.*, 1999). Therefore, one possible outcome of the heteromerization of SUR is generation of K_{ATP} channels with intermediate metabolic sensitivities. Our data support this idea. Compared to the T1+SUR2A (SUR1+SUR2A) channels, the azide-response of the T1+SUR1 (SUR1) channels was faster (shorter $t_{1/2}$ of activation), stronger (at all azide concentrations), and displayed a higher apparent affinity (Fig. 9). Since the SUR2A channels are insensitive to metabolic inhibition induced by azide, the response of the SUR1+SUR2A channels to metabolic inhibition is intermediate between those of the SUR1 and SUR2A channels. We predict that the metabolic sensitivities of all the possible SUR channels should follow this rank: SUR1>SUR1+SUR2B>SUR1+SUR2A>SUR2B> SUR2A+SUR2B>SUR2A channels.

The heteromerization of SUR also has important implication on the pharmacology of K_{ATP} channels. Among the many blockers and openers of K_{ATP} channels, several are already in clinical use: sulfonylurea blockers are common antidiabetics, and potassium channel openers such as diazoxide and nicorandil are used to treat hypertension, pectoris angina and PHHI (Touati *et al.*, 1998; Darendeliler *et al.*, 2002; Ashcroft, 2005; Jahangir and Terzic, 2005). These drugs bind primarily to SUR with subtype-specific affinities resulting in differential effects on the various types of K_{ATP} channels (Moreau *et al.*, 2005; Gribble and Reimann, 2002; Gribble and Reimann, 2003). In light of our finding, the composition of native K_{ATP} channels should be re-considered in those tissues coexpressing different SUR subtypes and the pharmacology of hybrid K_{ATP} channels should be characterized. This knowledge will be invaluable in designing new drugs targeting tissue-specific K_{ATP} channels and in guiding their administrations in order to minimize undesirable side effects.

Acknowledgements

We thank Drs. J Bryan for hamster SUR1, S Seino for rat SUR2A and mouse Kir6.2, FM Ashcroft for rat SUR2B and P Gros for human MRP1 clones. We are grateful to Drs. DE Logothetis and L Csanády for critical comments on this manuscript.

References

- Aguilar-Bryan L and Bryan J (1999) Molecular Biology of Adenosine Triphosphate-Sensitive Potassium Channels. *Endocr Rev* **20**:101-135.
- Ashcroft FM (2005) ATP-Sensitive Potassium Channelopathies: Focus on Insulin Secretion. *J Clin Invest* **115**:2047-2058.
- Babenko AP (2005) K_{ATP} Channels "Vingt Ans Apres": ATG to PDB to Mechanism. *J Mol Cell Cardiol* **39**:79-98.
- Babenko AP and Bryan J (2001) A Conserved Inhibitory and Differential Stimulatory Action of Nucleotides on Kir6.0/SUR Complexes Is Essential for Excitation-Metabolism Coupling by K_{ATP} Channels. *J Biol Chem* **276**:49083-49092.
- Babenko AP and Bryan J (2003) Sur Domains That Associate With and Gate K_{ATP} Pores Define a Novel Gatekeeper. *J Biol Chem* **278**:41577-41580.
- Babenko AP, Gonzalez G and Bryan J (1999) Two Regions of Sulfonylurea Receptor Specify the Spontaneous Bursting and ATP Inhibition of K_{ATP} Channel Isoforms. *J Biol Chem* **274**: 11587-11592.
- Babenko AP, Gonzalez G C and Bryan J (2000) Hetero-Concatemeric Kir6.x₄/SUR1₄ Channels Display Distinct Conductivities but Uniform ATP Inhibition. *J Biol Chem* **275**:31563-31566.
- Baron A, van Bever L, Monnier D, Roatti A and Baertschi A J (1999) A Novel K_{ATP} Current in Cultured Neonatal Rat Atrial Appendage Cardiomyocytes. *Circ Res* **85**:707-715.
- Chan KW, Wheeler A and Csanady L (2008) Sulfonylurea Receptors Type 1 and 2A Randomly Assemble to Form Heteromeric K_{ATP} Channels of Mixed Subunit Composition. *J Gen Physiol* **131**:43-58.

- Chan KW, Zhang H and Logothetis D E (2003) N-Terminal Transmembrane Domain of the SUR Controls Trafficking and Gating of Kir6 Channel Subunits. *EMBO J* **22**:3833-3843.
- Clement JP, Kunjilwar K, Gonzalez G, Schwanstecher M, Panten U, Aguilar-Bryan L and Bryan J (1997) Association and Stoichiometry of K_{ATP} Channel Subunits. *Neuron* **18**:827-838.
- Cui Y, Giblin J P, Clapp L H and Tinker A (2001) A Mechanism for ATP-Sensitive Potassium Channel Diversity: Functional Coassembly of Two Pore-Forming Subunits. *Proc Natl Acad Sci U S A* **98**:729-734.
- Dabrowski M, Larsen T, Ashcroft F M, Bondo H J and Wahl P (2003) Potent and Selective Activation of the Pancreatic Beta-Cell Type K_{ATP} Channel by Two Novel Diazoxide Analogues. *Diabetologia* **46**:1375-1382.
- Darendeliler F, Fournet J C, Bas F, Junien C, Gross M S, Bundak R, Saka N and Gunoz H (2002) ABCC8 (SUR1) and KCNJ11 (Kir6.2) Mutations in Persistent Hyperinsulinemic Hypoglycemia of Infancy and Evaluation of Different Therapeutic Measures. *J Pediatr Endocrinol Metab* **15**:993-1000.
- Fang K, Csanady L and Chan K W (2006) The N-Terminal Transmembrane Domain (TMD0) and a Cytosolic Linker (L0) of Sulphonylurea Receptor Define the Unique Intrinsic Gating of K_{ATP} Channels. *J Physiol* **576**:379-389.
- Giblin JP, Cui Y, Clapp L H and Tinker A (2002) Assembly Limits the Pharmacological Complexity of ATP-Sensitive Potassium Channels. *J Biol Chem* **277**:13717-13723.
- Gribble FM, Ashfield R, Ammala C and Ashcroft F M (1997) Properties of Cloned ATP-Sensitive K⁺ Currents Expressed in Xenopus Oocytes. *J Physiol* **498**:87-98.
- Gribble FM and Reimann F (2002) Pharmacological Modulation of K_{ATP} Channels. *Biochem Soc Trans* **30**:333-339.

- Gribble FM and Reimann F (2003) Sulphonylurea Action Revisited: the Post-Cloning Era. *Diabetologia* **46**:875-891.
- Inagaki N, Gonoi T, Clement J P, Namba N, Inazawa J, Gonzalez G, Aguilar-Bryan L, Seino S and Bryan J (1995) Reconstitution of $I_{K_{ATP}}$: an Inward Rectifier Subunit Plus the Sulfonylurea Receptor. *Science* **270**:1166-1170.
- Jahangir A and Terzic A (2005) K_{ATP} Channel Therapeutics at the Bedside. *J Mol Cell Cardiol* **39**:99-112.
- Karschin C, Ecke C, Ashcroft F M and Karschin A (1997) Overlapping Distribution of K_{ATP} Channel-Forming Kir6.2 Subunit and the Sulfonylurea Receptor SUR1 in Rodent Brain. *FEBS Lett* **401**:59-64.
- Liss B, Bruns R and Roeper J (1999) Alternative Sulfonylurea Receptor Expression Defines Metabolic Sensitivity of K_{ATP} Channels in Dopaminergic Midbrain Neurons. *EMBO J* **18**: 833-846.
- Masia R, Enkvetchakul D and Nichols C G (2005) Differential Nucleotide Regulation of K_{ATP} Channels by SUR1 and SUR2A. *J Mol Cell Cardiol* **39**:491-501.
- Matsuoka T, Matsushita K, Katayama Y, Fujita A, Inageda K, Tanemoto M, Inanobe A, Yamashita S, Matsuzawa Y and Kurachi Y (2000) C-Terminal Tails of Sulfonylurea Receptors Control ADP-Induced Activation and Diazoxide Modulation of ATP-Sensitive K^+ Channels. *Circ Res* **87**:873-880.
- Moreau C, Prost A L, Derand R and Vivaudou M (2005) SUR, ABC Proteins Targeted by K_{ATP} Channel Openers. *J Mol Cell Cardiol* **38**:951-963.
- Pountney DJ, Sun Z Q, Porter L M, Nitabach M N, Nakamura T Y, Holmes D, Rosner E, Kaneko M, Manaris T, Holmes T C and Coetzee W A (2001) Is the Molecular Composition of K_{ATP} Channels More Complex Than Originally Thought? *J Mol Cell Cardiol* **33**:1541-1546.

- Schwappach B, Zerangue N, Jan Y N and Jan L Y (2000) Molecular Basis for K_{ATP} Assembly: Transmembrane Interactions Mediate Association of a K^+ Channel With an ABC Transporter. *Neuron* **26**:155-167.
- Shi NQ, Ye B and Makielski J C (2005) Function and Distribution of the SUR Isoforms and Splice Variants. *J Mol Cell Cardiol* **39**:51-60.
- Shindo T, Yamada M, Isomoto S, Horio Y and Kurachi Y (1998) SUR2 Subtype (A and B)-Dependent Differential Activation of the Cloned ATP-Sensitive K^+ Channels by Pinacidil and Nicorandil. *Br J Pharmacol* **124**:985-991.
- Shyng S and Nichols C G (1997) Octameric Stoichiometry of the K_{ATP} Channel Complex. *J Gen Physiol* **110**:655-664.
- Thomzig A, Laube G, Pruss H and Veh R W (2005) Pore-Forming Subunits of K_{ATP} Channels, Kir6.1 and Kir6.2, Display Prominent Differences in Regional and Cellular Distribution in the Rat Brain. *J Comp Neurol* **484**:313-330.
- Touati G, Poggi-Travert F, Ogier d B, Rahier J, Brunelle F, Nihoul-Fekete C, Czernichow P and Saudubray J M (1998) Long-Term Treatment of Persistent Hyperinsulinaemic Hypoglycaemia of Infancy With Diazoxide: a Retrospective Review of 77 Cases and Analysis of Efficacy-Predicting Criteria. *Eur J Pediatr* **157**:628-633.
- Tricarico D, Mele A, Lundquist A L, Desai R R, George A L, Jr. and Conte C D (2006) Hybrid Assemblies of ATP-Sensitive K^+ Channels Determine Their Muscle-Type-Dependent Biophysical and Pharmacological Properties. *Proc Natl Acad Sci U S A* **103**:1118-1123.
- Yamada K and Inagaki N (2005) Neuroprotection by K_{ATP} Channels. *J Mol Cell Cardiol* **38**:945-949.

Yang K, Fang K, Fromondi L and Chan K W (2005) Low Temperature Completely Rescues the Function of Two Misfolded K_{ATP} Channel Disease-Mutants. *FEBS Lett* **579**:4113-4118.

Yokoshiki H, Sunagawa M, Seki T and Sperelakis N (1999) Antisense Oligodeoxynucleotides of Sulfonylurea Receptors Inhibit ATP-Sensitive K^+ Channels in Cultured Neonatal Rat Ventricular Cells. *Pflugers Arch* **437**:400-408.

Zerangue N, Schwappach B, Jan Y N and Jan L Y (1999) A New ER Trafficking Signal Regulates the Subunit Stoichiometry of Plasma Membrane K_{ATP} Channels. *Neuron* **22**:537-548.

Zingman LV, Hodgson D M, Bast P H, Kane G C, Perez-Terzic C, Gumina R J, Pucar D, Bienengraeber M, Dzeja P P, Miki T, Seino S, Alekseev A E and Terzic A (2002) Kir6.2 Is Required for Adaptation to Stress. *Proc Natl Acad Sci U S A* **99**:13278-13283.

Footnotes

We thank Drs. J Bryan for hamster SUR1, S Seino for rat SUR2A and mouse Kir6.2, FM Ashcroft for rat SUR2B and P Gros for human MRP1 clones. We are grateful to Drs. DE Logothetis and L Csanády for critical comments on this manuscript.

This work was supported by NIH grant DK60104 (to KWC). TM is supported by a Beginning Grant-in-Aid from the American Heart Association (0765275U).

Present address for KWC: Department of Pharmacological Sciences, CV Therapeutics, 1651 Page Mill Road, Palo Alto, CA 94304, USA

Present address for KY: Department of Pediatrics, Case Western Reserve University, School of Medicine Rainbow Babies and Children's Hospital, 11100 Euclid Ave, Cleveland OH 44106-6011, USA

Present address for KF: Departments of Physiology and Medicine and the Cardiovascular Research Laboratories, MRL 3-609, David Geffen School of Medicine at UCLA, Los Angeles, CA 90095-1760, USA

Figure legends:

Fig. 1. Presence of both SUR1 and SUR2A in the same channel complex. A-C, crude membrane preparations from oocytes expressing different proteins, as indicated at the top of panel A, were run on SDS-PAGE for Western blot analyses (8, 6 and 12 % gels, respectively). Western blots showing the expression of FLAG-tagged SUR1 (F-SUR1), HA-tagged SUR1 and SUR2A and GFP-tagged Kir6.2 (Kir6.2-GFP) are shown in A-C, respectively. D-E, Western blots showing the coprecipitations of SUR1 and SUR2A and Kir6.2GFP, respectively, when F-SUR1 was immunoprecipitated. Protein samples were run on 8% and 12% gels, respectively. Note that the control from uninjected oocytes (lane 5 from the left) was not included in the Western blot shown in A.

Fig. 2. Using two triple tandems to study the coassembly of different SUR subtypes. A, each triple tandem, T1 or T2, comprises one SUR (SUR1 or SUR2A) and two Kir6.2 Δ 26 connected by two glycine-linkers, L. T1 and T2 were expressed alone or with different SUR subtypes (SUR1 or SUR2A or 2B) in *Xenopus* oocytes and the resulting currents were characterized and compared. T1(I-AAA) and T1(II-AAA) have the dominant negative pore mutations (GFG \rightarrow AAA) in cassette I and cassette II, respectively. B-C, the possible molecular configurations of the functional channels formed when T1 or T2 is expressed alone and with SUR2 or SUR1. In B, each individual triple tandem is differently shaded.

Fig. 3. Coexpression of T1 with different SUR subtypes indicates that SUR1 can associate with SUR2A and SUR2B. A-D, time courses of the whole-cell currents recorded at -80 mV from oocytes expressing T1 alone (A), T1+SUR1 (B), T1+SUR2A (C) and T1+SUR2B (D). At the start of the recordings, the oocytes were superfused with the 96K bath solution. Sodium azide, diazoxide, pinacidil, glibenclamide and barium chloride were then sequentially introduced into the bath solution as indicated by the colored bars. I_{ba} (basal current), I_{az} (azide-activated current), I_{dzo} (diazoxide-activated current), I_{pin} (pinacidil-activated current) and I_{tot} (total current) are defined in the figures. E, bar-chart plots of the basal, activated and total currents obtained from oocytes expressing T1, T1+SUR1, T1+SUR2A and T1+SUR2B. The activated currents include azide- and diazoxide-activated currents. For T1+SUR2A, pinacidil-activated currents

were also measured and presented. The total current is the sum of the basal and all the activated currents (i.e. $I_{\text{tot}} = I_{\text{ba}} + I_{\text{az}} + I_{\text{dZX}} + I_{\text{pin}}$; for channels that are not activated by pinacidil, $I_{\text{tot}} = I_{\text{ba}} + I_{\text{az}} + I_{\text{dZX}}$).

Fig. 4. Physical association between T1 and SUR1 or SUR2A. A, Western blot showing the expression of SUR1, T1, T1+SUR1 and T1+SUR2A. Both SUR1 and T1 contain a FLAG-epitope at their N-termini. Notice the presence of two higher MW bands for SUR1 and one for T1 (indicated by *). B, Western blot showing the expression of SUR1 and SUR2A when coexpressed with T1. C, Western blot showing the presence of SUR1 and SUR2A after the immunoprecipitation of T1. Immunoprecipitations were performed using the anti-FLAG antibody. SUR1 and SUR2A used in this experiment were tagged with an HA-epitope. Protein samples were resolved on 6% (A) or 8% (B-C) SDS-PAGE.

Fig. 5. Incorporation of SUR2A into T1 results in longer burst durations. A, representative single-channel recordings for T1 and T1+SUR2A. The dotted lines correspond to the zero current levels. Channel openings are in the downward direction. The mean burst duration for T1 was increased ~2-fold in the presence of SUR2A (Table 2). B, the single-channel closed times and open dwell times were fitted by maximum likelihood with sums of exponential functions. For both channels, the closed and open times were best fitted with four and one exponentials, respectively. The values of the fit parameters (see Methods for the definition of the symbols) are shown in the panels.

Fig. 6. Coexpression of T2 with different SUR subtypes indicates that SUR2A can associate with SUR1 and SUR2B. A-D, time courses of the whole-cell currents recorded at -80 mV from oocytes expressing T2 alone (A), T2+SUR1 (B), T2+SUR2A (C) and T2+SUR2B (D). The colored bars indicate the presence of the various drugs/compounds in the 96K bath solution. The color coding is the same as in Figure 2. I_{tot} for each channel is defined in the figure. E, bar-chart plots of the basal, activated and total currents obtained from oocytes expressing T2, T2+SUR1, T2+SUR2A and T2+SUR2B. The total current is the sum of the basal and all the activated currents (i.e. $I_{\text{tot}} = I_{\text{ba}} + I_{\text{az}} + I_{\text{dZX}} + I_{\text{pin}}$).

Fig. 7. SUR1 and SUR2A can also coassemble in a mammalian heterologous system to form channels with mixed pharmacology. A-C, time courses of the whole-cell currents recorded at -80 mV from COS-7 cells expressing T1 alone (A), T1+SUR1 (B), T1+SUR2A (C). The colored bars indicate the presence of

various drugs in the HK bath solution, as indicated. I_{ba} (basal current), I_{dzx} (first application of diazoxide), I_{pin} (first application of pinacidil) and I_{tot} (total current) are defined in the figures. D, bar-chart plots of the basal, drug-activated and total currents obtained from COS-7 cells expressing T1, T1+SUR1 and T1+SUR2A. The total current is the sum of the basal and all the activated currents (i.e. $I_{tot}=I_{ba}+I_{dzx}+I_{pin}$; for channels that are not activated by pinacidil, $I_{tot}=I_{ba}+I_{dzx}$).

Fig. 8. Coexpression of T1 leads to the surface localization of both SUR1 and SUR2A in HEK-293 cells. SUR1 and SUR2A were tagged with HA epitope and images from cells immunostained with an anti-HA primary and Alexa Fluor 594-conjugated secondary antibody are shown. The differential interference contrast (DIC) image is superimposed to outline the perimeters of the cells. A-D, immunostaining of SUR1 or SUR2A in the absence or presence of T1. When expressed alone, both SUR1 (A) and SUR2A (C) were localized to intracellular compartments (likely the ER). Coexpression of T1 led to the surface expression of SUR1 (B) and SUR2A (D). E-F, images from cells transfected with empty vector (pcDNA3) alone (E) and T1+SUR2A where the primary antibody was excluded in the staining procedure (F) are shown as negative controls.

Fig. 9. Heteromeric K_{ATP} channels comprising both SUR1 and SUR2A show intermediate responses to metabolic inhibition. A, normalized time courses comparing the rate of azide activation for T1+SUR1, T1+SUR2A and T1+SUR2B channels. Maximum azide-activated currents were used to normalize the three time courses. Oocytes were superfused with 96K solution and 3 mM azide and 10 μ M glibenclamide were added as indicated by the bars. B, normalized time courses of currents obtained at -80 mV from oocytes expressing T1+SUR1 (shown in red) and T1+SUR2A (black). Maximum total currents were used for normalization. Azide (1 mM and 5 mM) was added to the bath solution as indicated by the arrows. Ba^{2+} (3 mM) was added at the end of the experiments.

TABLE 1

Summary of the basal, activated and total currents from T1 and T2 alone, and when coexpressed with different SUR subtypes in *Xenopus* oocytes

Basal, azide-, diazoxide-, pinacidil-activated and total currents were defined in Figures 3 and 6; n=number of experiments; numbers in parentheses represent the percentages of the indicated currents relative to the corresponding total currents

	Basal (μA)	Az-activated (μA)	Dzx-activated (μA)	Pin-activated (μA)	Glib-sensitive (μA)	Total (μA)	n
T1	-0.80 ± 0.05 (27.09 \pm 4.41 %)	-1.09 ± 0.25 (27.99 \pm 3.60 %)	-1.81 ± 0.48 (44.92 \pm 4.24 %)		-2.63 ± 0.62 (67.29 \pm 3.24 %)	-3.70 ± 0.72	8
T1+SUR1	-4.72 ± 0.43 (16.77 \pm 2.38 %)	-16.37 ± 1.92 (53.68 \pm 2.83 %)	-10.15 ± 2.75 (29.55 \pm 3.82 %)		-28.34 ± 4.58 (89.71 \pm 1.25 %)	-31.24 ± 4.64	8
T1+SUR2A	-1.37 ± 0.27 (4.25 \pm 0.62 %)	-5.36 ± 0.88 (16.94 \pm 1.79 %)	-6.63 ± 1.78 (18.87 \pm 2.93 %)	-18.69 ± 2.67 (59.94 \pm 3.09 %)	-27.37 ± 4.56 (85.24 \pm 1.47 %)	-32.04 ± 5.21	8
T1+SUR2B	-1.60 ± 0.20 (8.36 \pm 1.24 %)	-8.00 ± 1.25 (37.31 \pm 2.98 %)	-11.04 ± 1.13 (54.33 \pm 2.45 %)		-14.99 ± 1.50 (74.14 \pm 3.45 %)	-20.63 ± 2.27	8
T1+MRP1	-0.19 ± 0.17 (11.00 \pm 8.75 %)	-0.81 ± 0.11 (42.86 \pm 4.56 %)	-0.92 ± 0.07 (49.32 \pm 3.06 %)		-1.03 ± 0.14 (54.46 \pm 5.77 %)	-1.87 ± 0.11	5
T2	-0.87 ± 0.08 (13.04 \pm 1.19 %)	-0.14 ± 0.05 (2.09 \pm 0.72 %)	-0.46 ± 0.05 (6.74 \pm 0.55 %)	-5.21 ± 0.20 (78.13 \pm 1.06 %)	-4.16 ± 0.23 (62.36 \pm 2.69 %)	-6.68 ± 0.24	7
T2+SUR1	-1.56 ± 0.32 (2.77 \pm 0.98 %)	-6.28 ± 1.35 (7.52 \pm 1.00 %)	-11.02 ± 1.59 (15.16 \pm 1.96 %)	-61.28 ± 12.57 (74.55 \pm 2.14 %)	-76.45 ± 14.47 (95.15 \pm 0.62 %)	-80.13 ± 14.87	7
T2+SUR2A	-0.53 ± 0.15 (2.71 \pm 0.92 %)	-0.08 ± 0.06 (0.57 \pm 0.36 %)	-0.27 ± 0.05 (1.67 \pm 0.42 %)	-17.48 ± 1.69 (95.05 \pm 0.58 %)	-15.97 ± 1.55 (86.84 \pm 2.15 %)	-18.36 ± 1.73	9
T2+SUR2B	-0.95 ± 0.24 (7.28 \pm 1.51 %)	-0.22 ± 0.12 (2.76 \pm 1.42 %)	-0.98 ± 0.11 (8.44 \pm 0.51 %)	-10.10 ± 1.73 (81.52 \pm 1.32 %)	-8.53 ± 1.39 (69.09 \pm 2.72 %)	-12.25 ± 1.96	7

TABLE 2

Single-channel parameters for T1 and T1+SUR2A

γ , single channel conductance; P_o , open probability; τ_{ci} and a_{ci} , the time constant and the fractional contribution of the i^{th} closed time component, respectively; N , the number of channel closures within a burst; τ_b and τ_{ib} , the burst and interburst duration, respectively; n , number of experiments.

	T1	T1+SUR2A
γ (pS)	58.36 ± 1.75	58.54 ± 1.20
P_o	0.74 ± 0.05	0.80 ± 0.04
τ_{c1} (ms)	0.19 ± 0.01	0.19 ± 0.01
τ_{c2} (ms)	1.56 ± 0.20	1.86 ± 0.39
τ_{c3} (ms)	9.31 ± 1.14	11.14 ± 3.24
τ_{c4} (ms)	2722 ± 1162	2594 ± 706
a_{c1} (%)	98.04 ± 0.53	99.27 ± 0.10
a_{c2} (%)	1.54 ± 0.44	0.49 ± 0.08
a_{c3} (%)	0.39 ± 0.08	0.23 ± 0.05
a_{c4} (%)	0.031 ± 0.016	0.011 ± 0.006
τ_o (ms)	1.53 ± 0.06	1.58 ± 0.03
N	69.07 ± 16.31	156.70 ± 21.94
τ_{ib} (ms)	3.17 ± 0.29	3.90 ± 0.36
τ_b (ms)	123.30 ± 29.67	280.48 ± 41.04
n	6	8

FIGURE 1

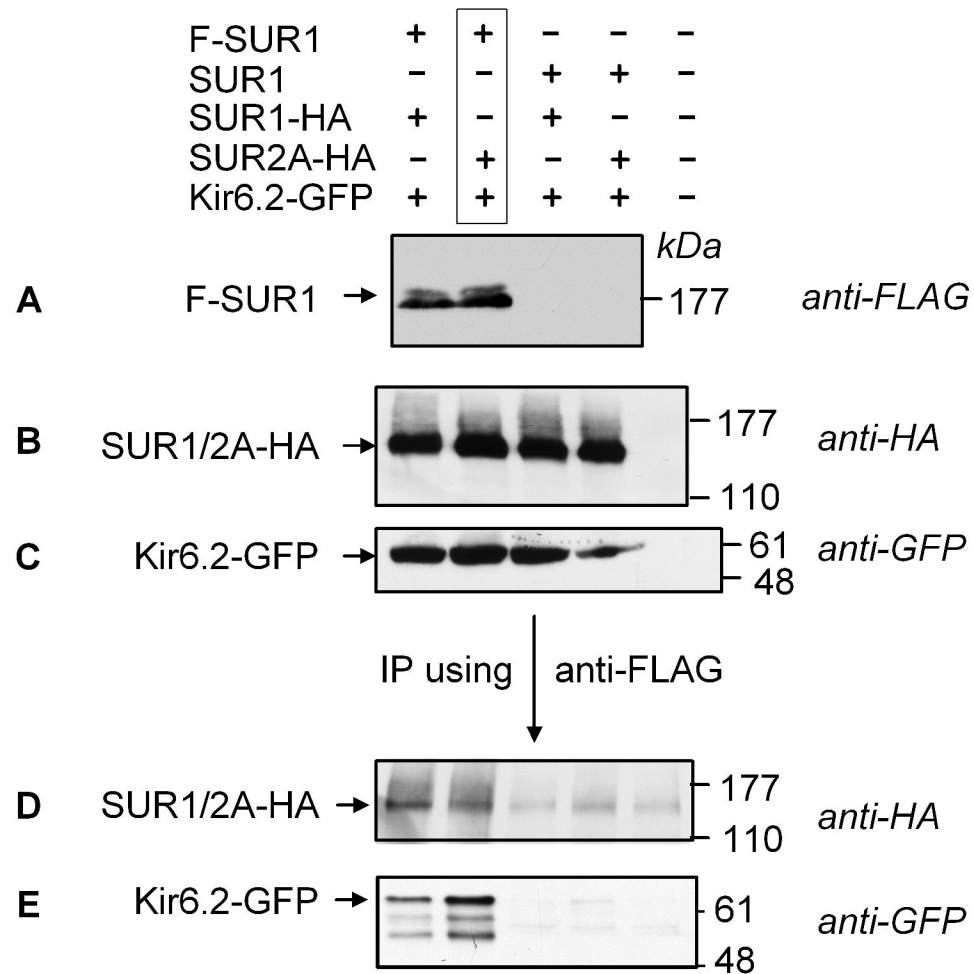


FIGURE 2

A

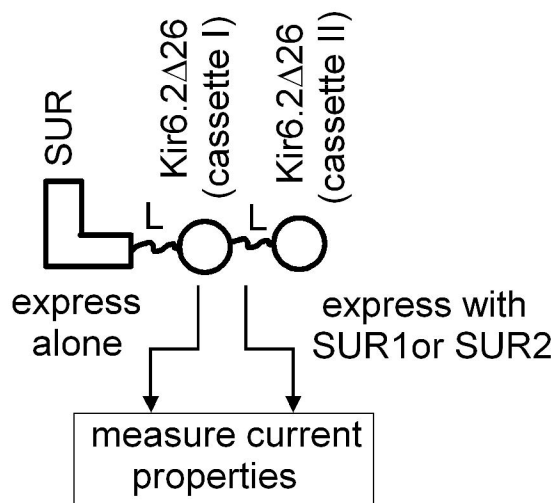
Triple Tandem Construct (T)

$T1 = SUR1 - Kir6.2\Delta26 - Kir6.2\Delta26$

$T2 = SUR2A - Kir6.2\Delta26 - Kir6.2\Delta26$

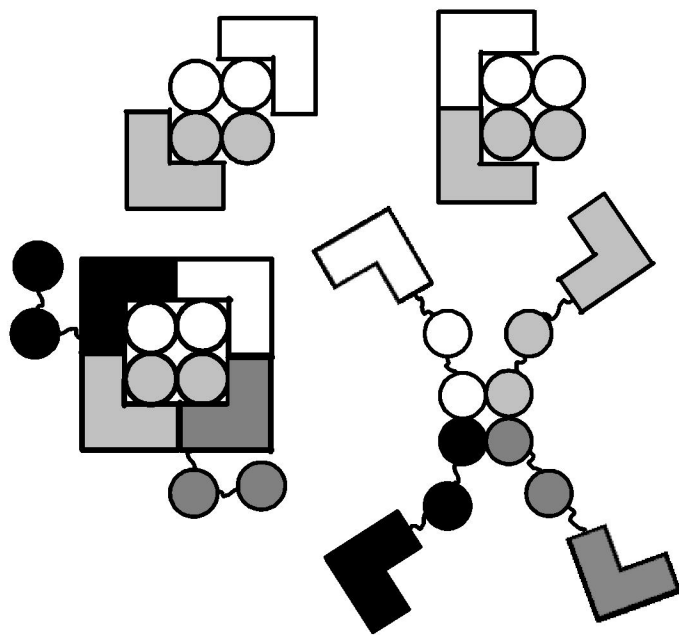
$T1(I-AAA) = SUR1 - Kir6.2\Delta26(GFG \rightarrow AAA) - Kir6.2\Delta26$

$T1(II-AAA) = SUR1 - Kir6.2\Delta26 - Kir6.2\Delta26(GFG \rightarrow AAA)$



B

T1 or T2 expressed alone



C

T1+SUR2 or T2+SUR1

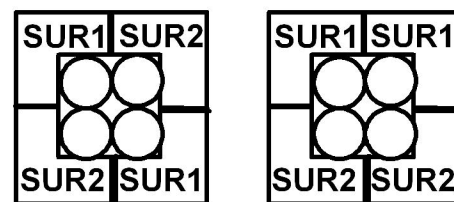


FIGURE 3

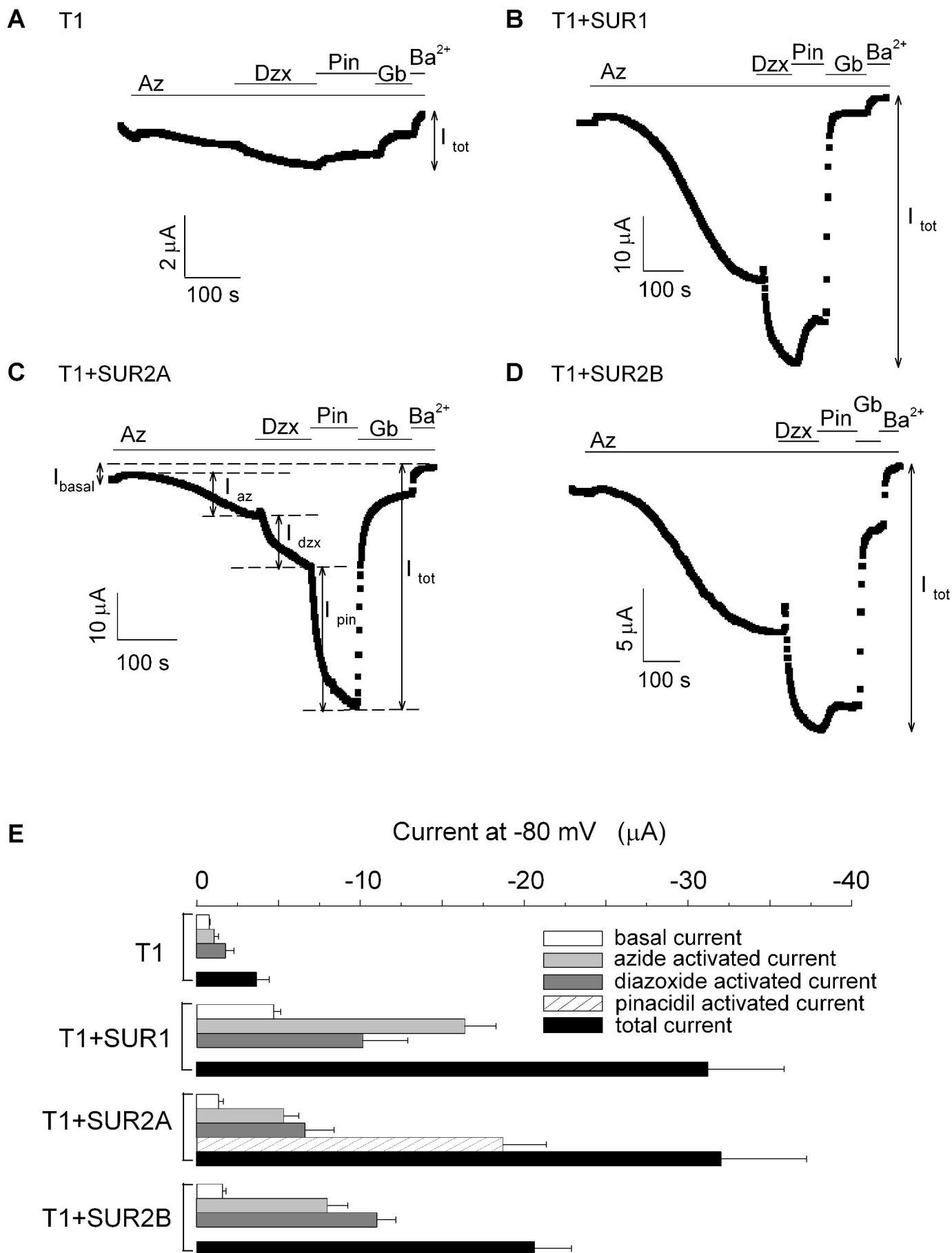


FIGURE 4

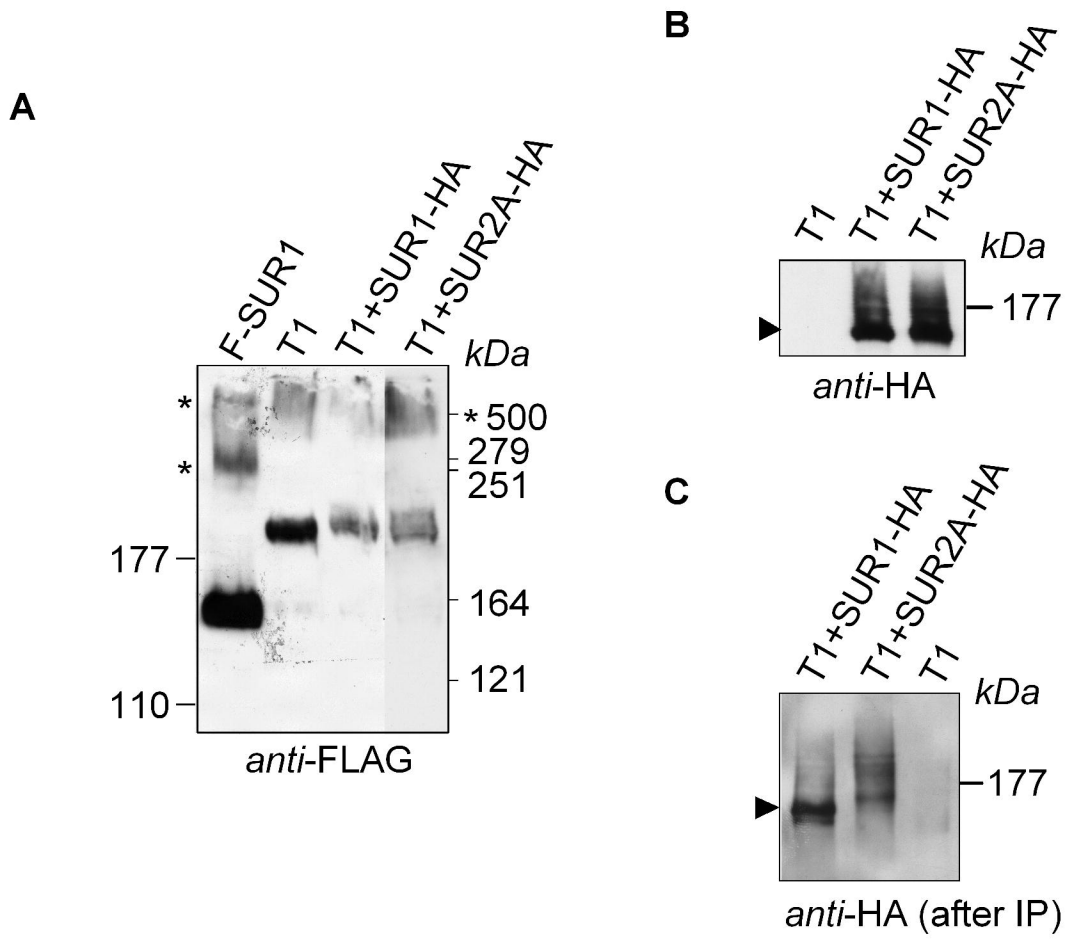


FIGURE 5

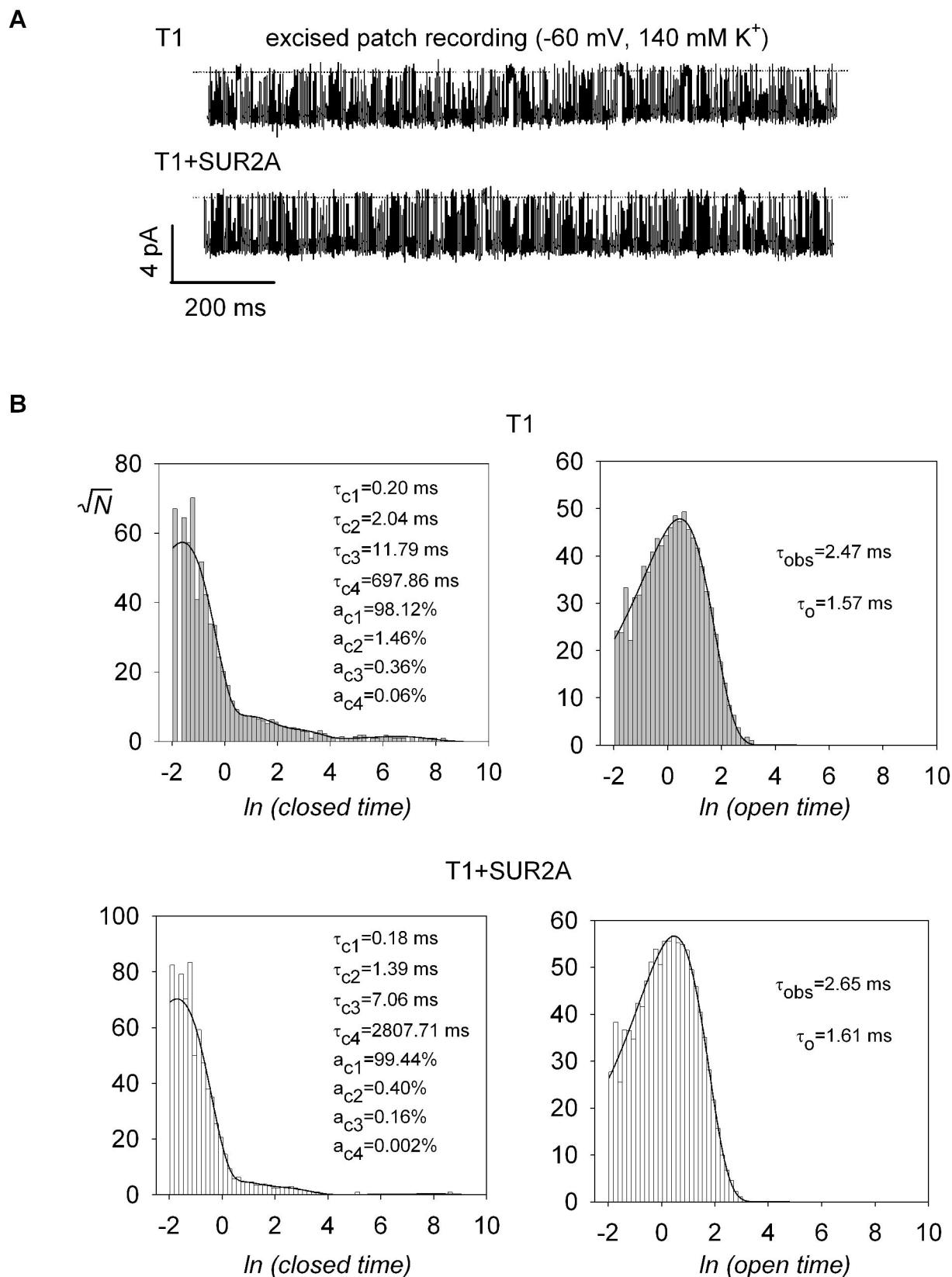


FIGURE 6

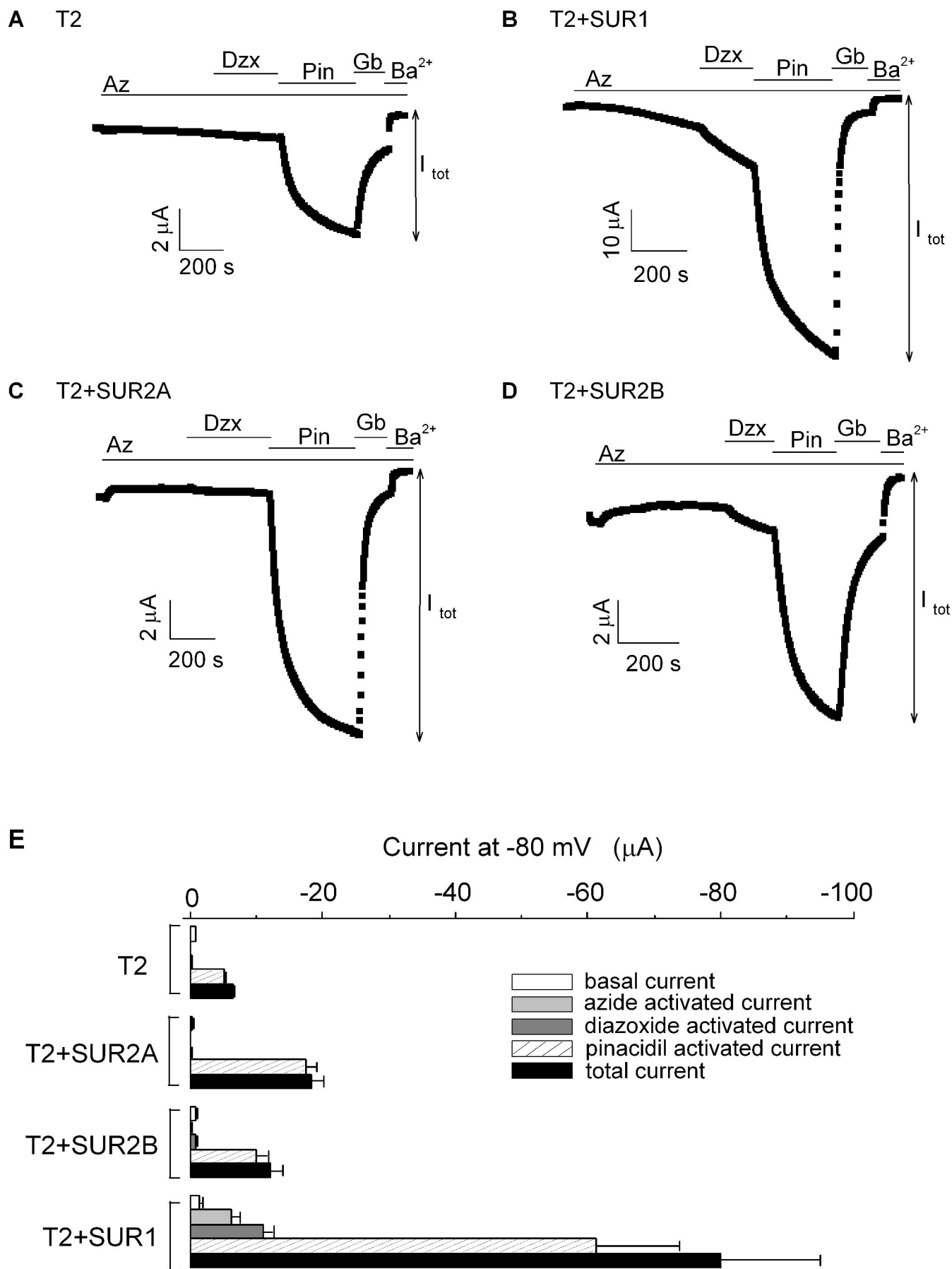
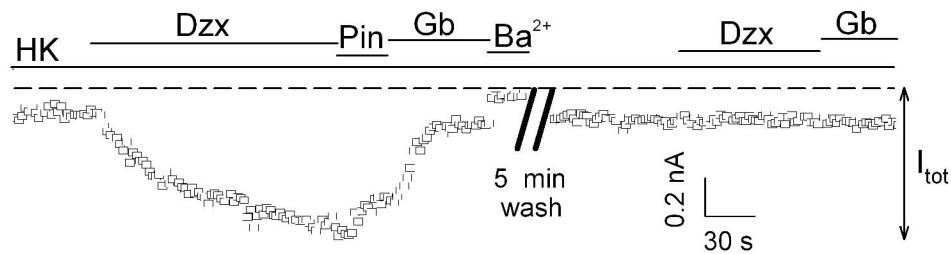
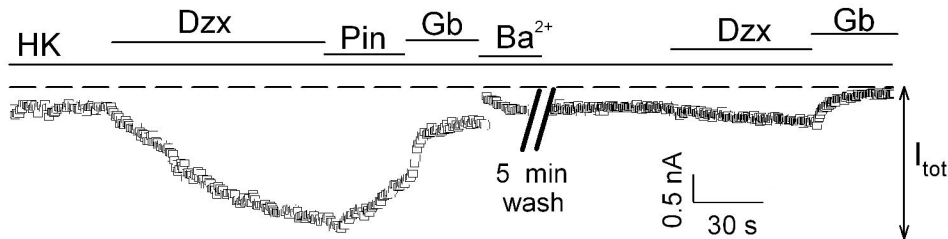


FIGURE 7

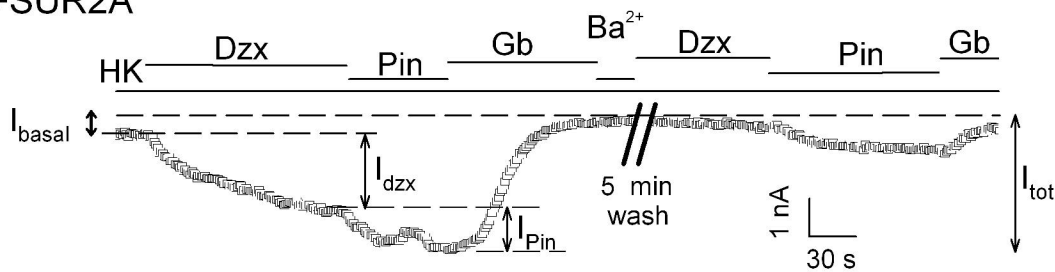
A T1



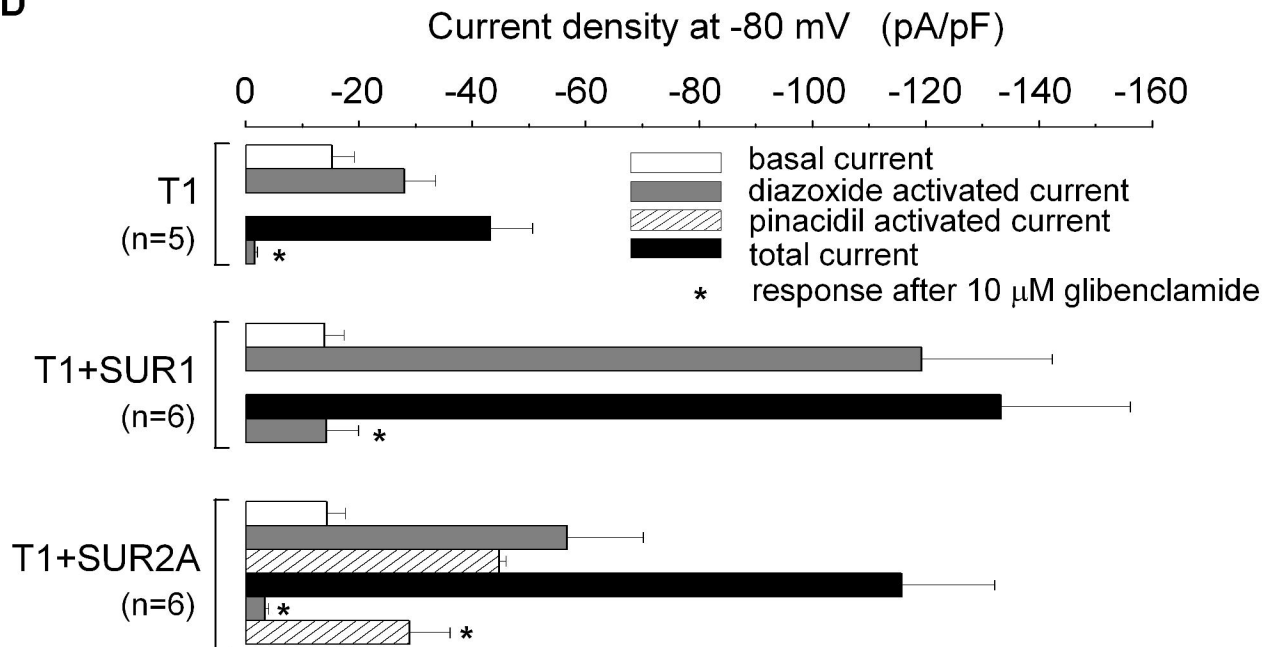
B T1+SUR1



C T1+SUR2A



D



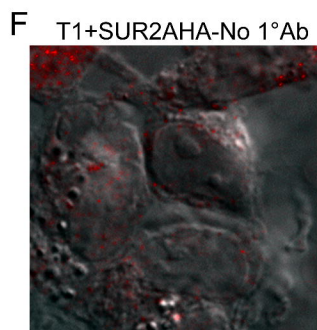
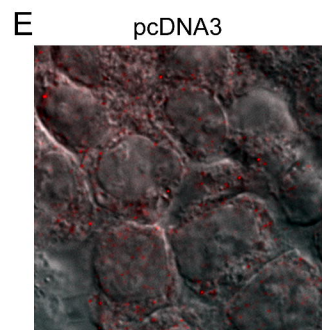
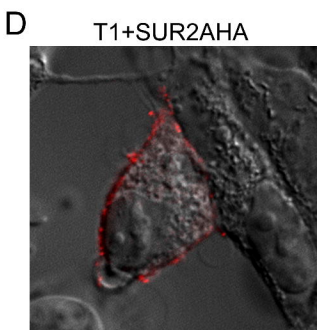
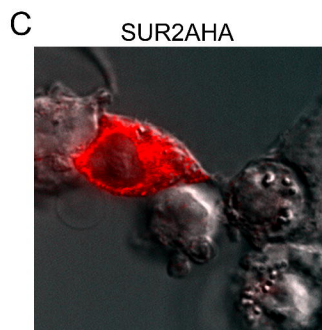
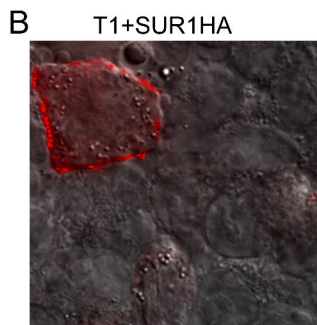
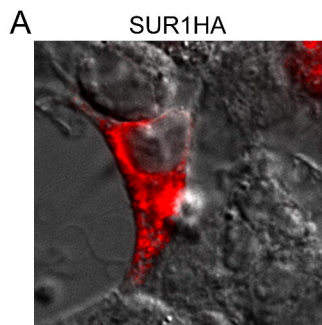
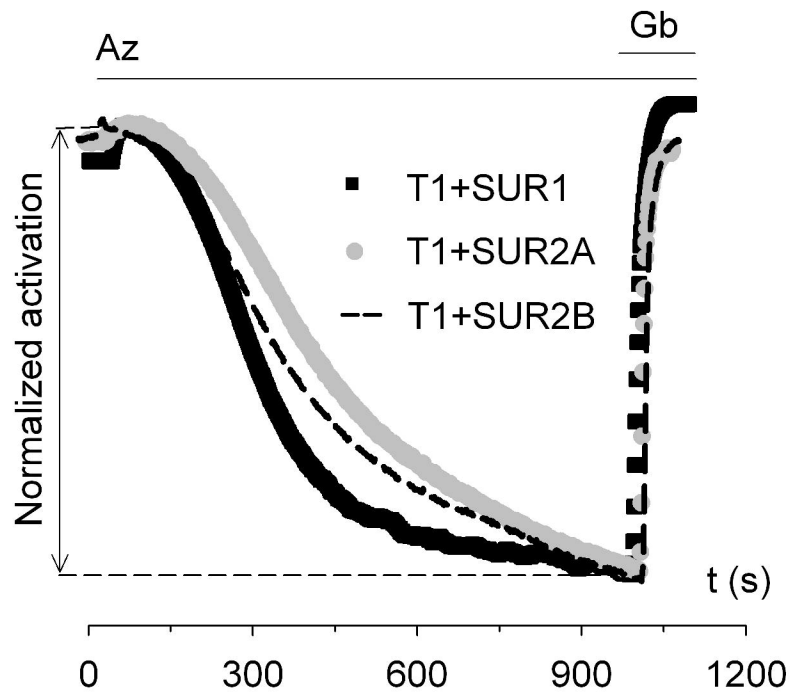


FIGURE 9

A



B

